Supporting information for

Pre-engineering artificial solid electrolyte interphase for hard carbon anodes for superior sodium storage performance

Lu Shi,[a] Yadi Sun,[a] Wei Liu,[a] Fanjun Zhao,[a] Ruixin Liu, [a] Chengyu Dong,[b,*] Guanggui Cheng,[a] and Jianning Ding [a,c,*]

[a] Institute of Intelligent Flexible Mechatronics & School of Mechanical Engineering, Jiangsu University, Zhenjiang, 212013, China

[b] College of Engineering, Nanjing Agricultural University, 40 Dianjiangtai Road, Nanjing, 210031, China

[c] School of Mechanical Engineering, Yangzhou University, Yangzhou, 225009, China.

[*] Corresponding authors.

E-mail addresses: dongchengyu@njau.edu.cn (Chengyu Dong), dingjn@ujs.edu.cn (Jianning Ding)

Experimental

Sample preparation

3.6 g of the commercial hard carbon (HC) particles (Taobao store) and 0.6 g of dopamine hydrochloride were dispersed into tris buffer solution (10 mM, pH 8.5) under ultrasonication. After the polymerization of dopamine on the surface of the commercial HC particles for 24 h, the HC/polydopamine composite was obtained. Next, the HC/polydopamine particles were pyrolyzed under Ar at 400 ^{o}C for 2 h, and then heated up to 1000 ^{o}C for 2 h with the heating rate of 5 ^{o}C min^{-1}. The final product was named as HC@C. When the mass ratio of the commercial HC particles to dopamine hydrochloride was adjusted to 3/1 and 12/1, the obtained samples were denoted as HC@C-3 and HC@C-12, respectively.

Structural characterization

The microstructure and morphology of the as-prepared samples were observed by FESEM (JSM-6700F) and TEM (JEOJ JEM-2100F). Raman spectra were conducted using Thermo Fischer DXR Raman spectroscopy with 532 nm laser. XRD tests were characterized on Bruker D8 with Cu Kα radiation in the range of 10°-80° with a scan rate of 4° min^{-1} (λ = 0.154 nm). XPS was performed on ESCALAB 250Xi spectrometer with Al Kα radiation.

Electrochemical measurements

The prepared active material and sodium alginate (95 wt%:5 wt%) were mixed in DI water to make the slurry. The slurry was pasted on the Cu foil and then completely dried at 100 °C for 12 h in the vacuum oven. The mass loading of active materials is about 2-3 mg cm^{-2}. CR2032-type coin cells were assembled in the glovebox with the electrode sheet, separator (glass fiber, Whatman GF/F) and Na metal. The employed electrolyte was 1 M $NaPF_6$ in DEGDME. The cycling performance, rate capability under different current densities and galvanostatic intermittent titration technique (GITT) tests were conducted on a LAND CT2001A battery system within 0-2 V. Electrochemical impedance spectroscopy (EIS) were examined from 0.01 to10^5 Hz on a CHI660E electrochemical workstation. GITT was studied with a pulse current of 30 mA g^{-1} for 0.5 h and interval time of 2 h. The diffusivity coefficient of Na^+ (D_{Na+}) can be calculated based on the following equation.

$$D_{Na+} = \frac{4}{\pi\tau}\left(\frac{m_B V_M}{M_B S}\right)^2\left(\frac{\Delta E_S}{\Delta E_\tau}\right)^2 \quad (1)$$

Where m_B, V_M and M_B are the active mass, molar volume and molar mass of carbon. τ refers to the pulse duration. S stands for the area of the electrodes. ΔE_s and ΔE_τ can

be obtained from the GITT curves, indicating two adjacent stable potential difference and the voltage shift caused by impulse current.

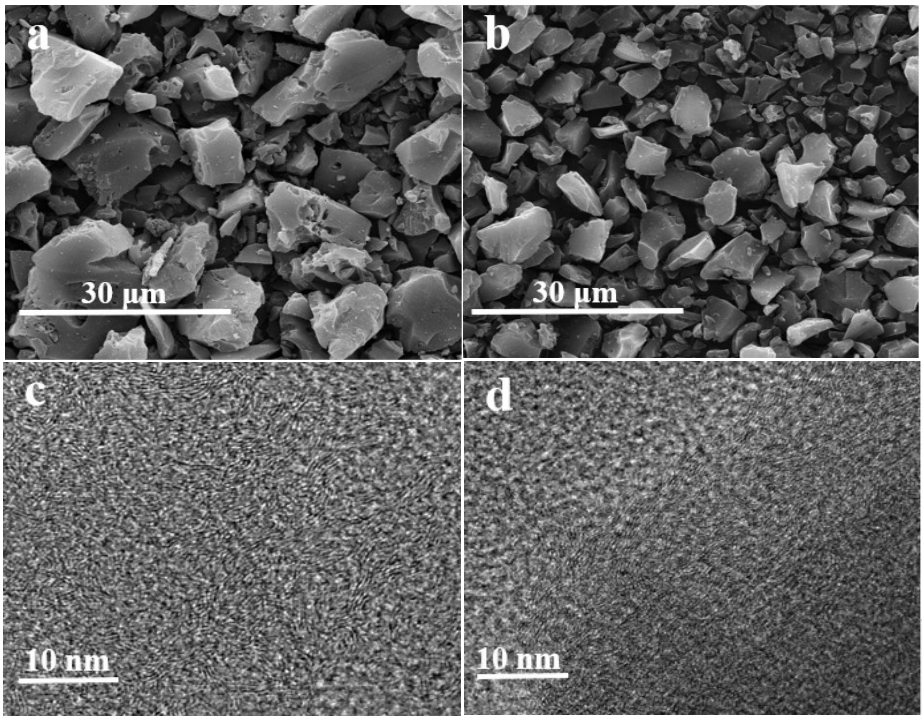

Fig. S1 SEM images of HC (a) and HC@C (b); HRTEM images of HC (c) and HC@C (d).

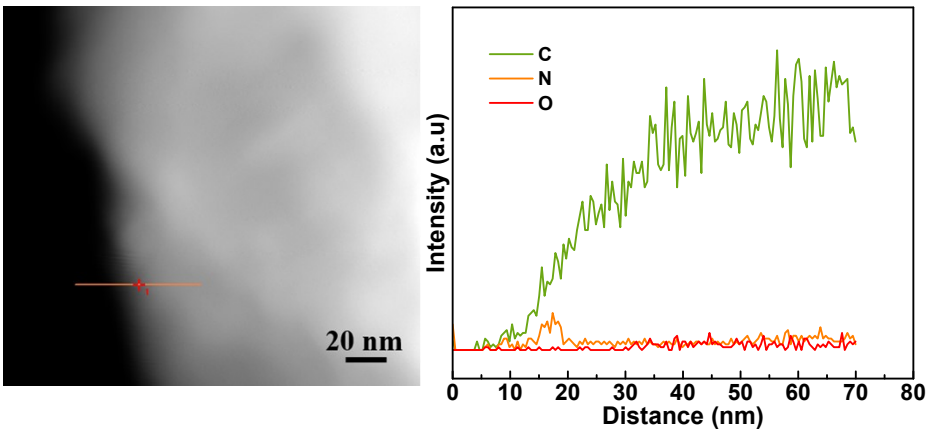

Fig. S2 TEM image and the corresponding line scanning of HC@C.

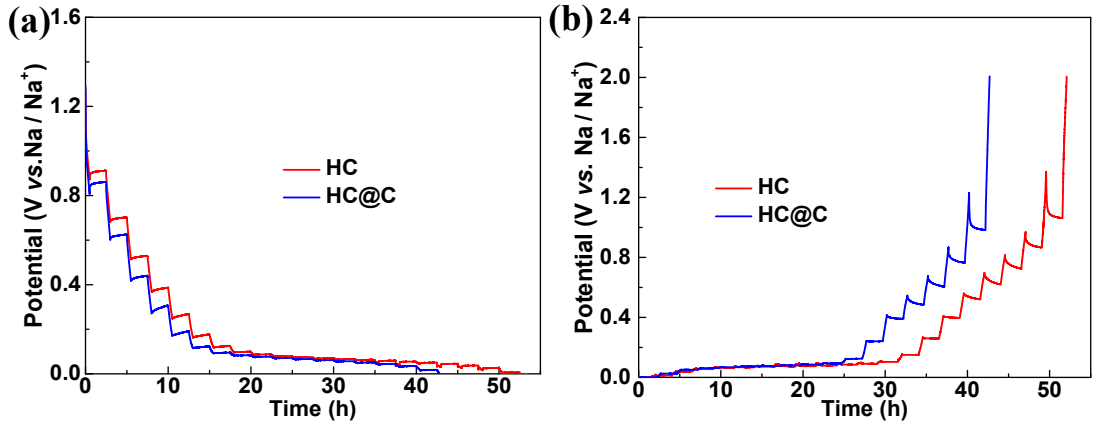

Fig. S3 GITT potential profiles in the sodiation (a) and desodiation processes (b) for HC and HC@C.

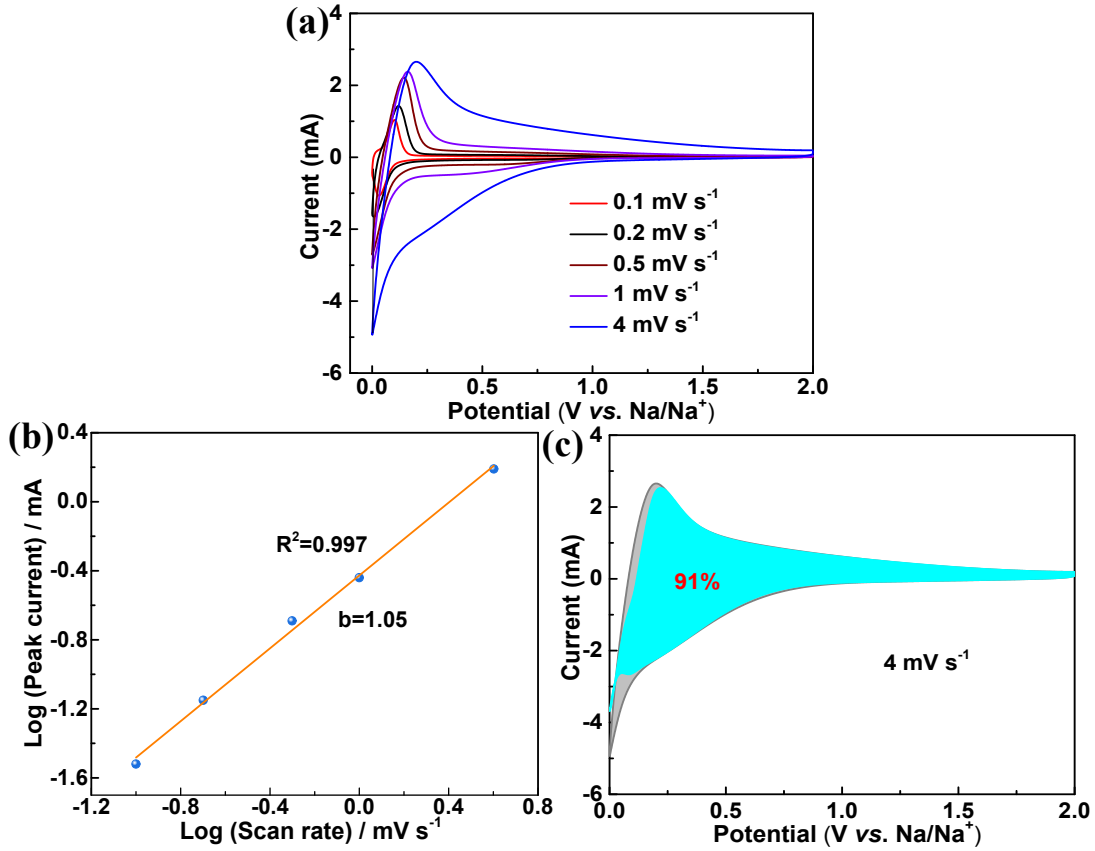

Fig. S4 (**a**) CV curves of HC@C at the various scan rates from 0.1-4 mV s^{-1}; (**b**) Log i versus log v plots; (**c**) The capacitive contribution diagram at 4 mV s^{-1} of HC@C.

$$i = av^b \tag{2}$$

where i represents the current (mA) and v stands for the scan rate (mV s^{-1}).

$$i = k_1 v + k_2 v^{1/2} \tag{3}$$

Where k_1v represents the capacitive process and k_2v corresponds to the diffusion process.

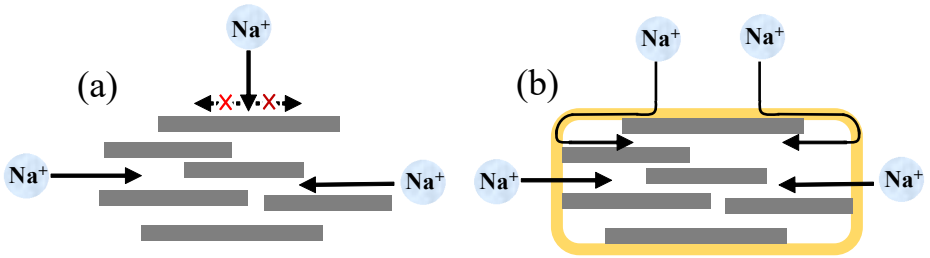

Fig. S5 Scheme of Na^+ diffusion into different hard carbon anodes. (a) Na^+ diffusion into HC from only the edge side; (b) HC@C can provide 3D Na^+ diffusion paths and additional entrance at the basal plane by the coated carbon layer.

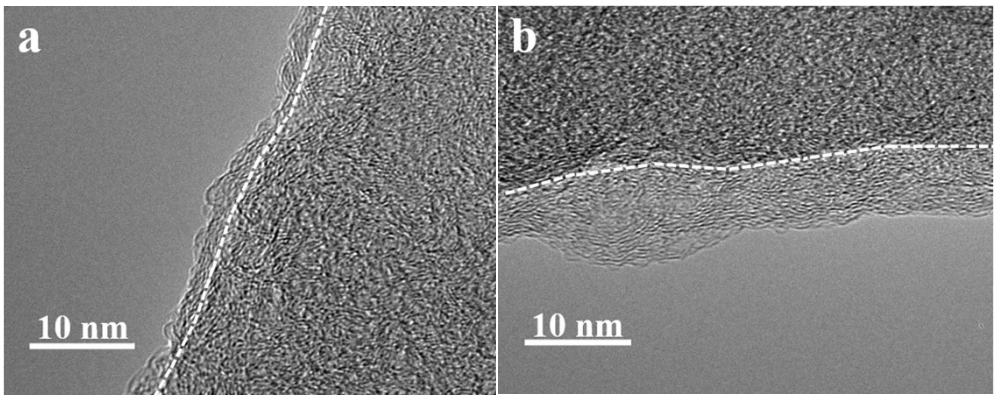

Fig. S6 TEM images of HC@C-12 (a) and HC@C-3 (b).

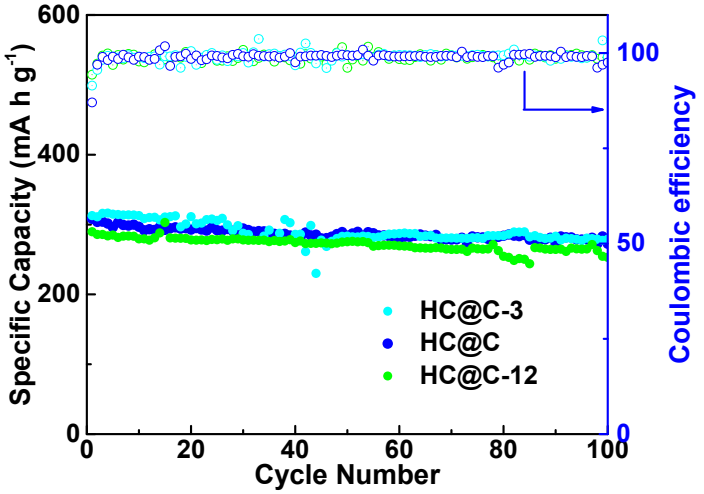

Fig. S7 Cycling performance of the series of HC@C samples fabricated with different mass ratios of dopamine hydrochloride.

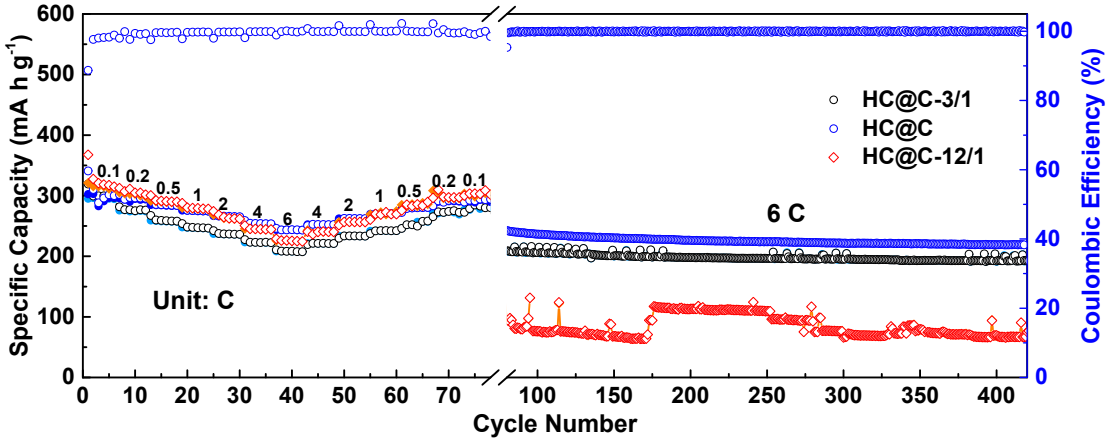

Fig. S8 Rate performance of the series of HC@C samples fabricated with different mass ratios of dopamine hydrochloride from 0.1 C to 6 C.

Table S1 Comparison of both the ICE and high-rate sodium storage properties between HC@C with the pre-engineering SEI and the recently reported hard carbon materials.

Materials	ICE /%	Reversible Capacity/mA h g^{-1}	Current Density /mA g^{-1}	Ref.
ZnO-assisted bulk etching hard carbon	77.63	344	2000	18
Vanadium-modified hard carbon spheres	68.7	68	1000	19

PF/GO-derived carbon	90.4	73	600	20
Phenolic resin and lignin derived hard carbon	87	205	1800	14
Boron-doped hard carbon nanospheres	65.4	75	2000	21
Hard carbon with micropores inside	80.6	125	2000	22
Hard carbon nanofibers	53	69	2000	23
Pitch and resin-derived hard carbon	60.9	264.5	2000	5
C=O bonded hard carbon	93.2	110	2000	24
Al_2O_3 modified hard carbon	81.1	83.6	1000	7
MgO-templated hard carbon	88	350	2500	25
Commercial hard carbon with surface oxygenated functionalities	77	70	2000	26
Artificial SEI modified hard carbon	94	246 (Rate performance test)	1800	This work

Appropriate amount of phenolic resin has been employed as the carbon source to fabricate the carbon-coated hard carbon without nitrogen-doping under the same carbonation process. The corresponding electrochemical performance are shown in Fig. S9, including the initial galvanostatic charge/discharge curves, the cycling performance at 0.1 C, the rate performance and the long-term cycling stability at 1 C. As shown in Fig. S9, it shows a lower initial Coulombic efficiency of 85% and delivers a reversible capacity of 261 mA h g^{-1} at 0.1 C after 100 cycles. When cycled at the current density of 1 C, the capacity starts to fade after 670 cycles, showing unsatisfied cycling stability. When the current density increases from 0.1 C to 6 C, the reversible capacity maintains around 205 mA h g^{-1}. Compared with that of HC@C with nitrogen-doped carbon coating from polydopamine, the carbon-coated hard carbon with phenolic resin without nitrogen-doping shows poor electrochemical performance.

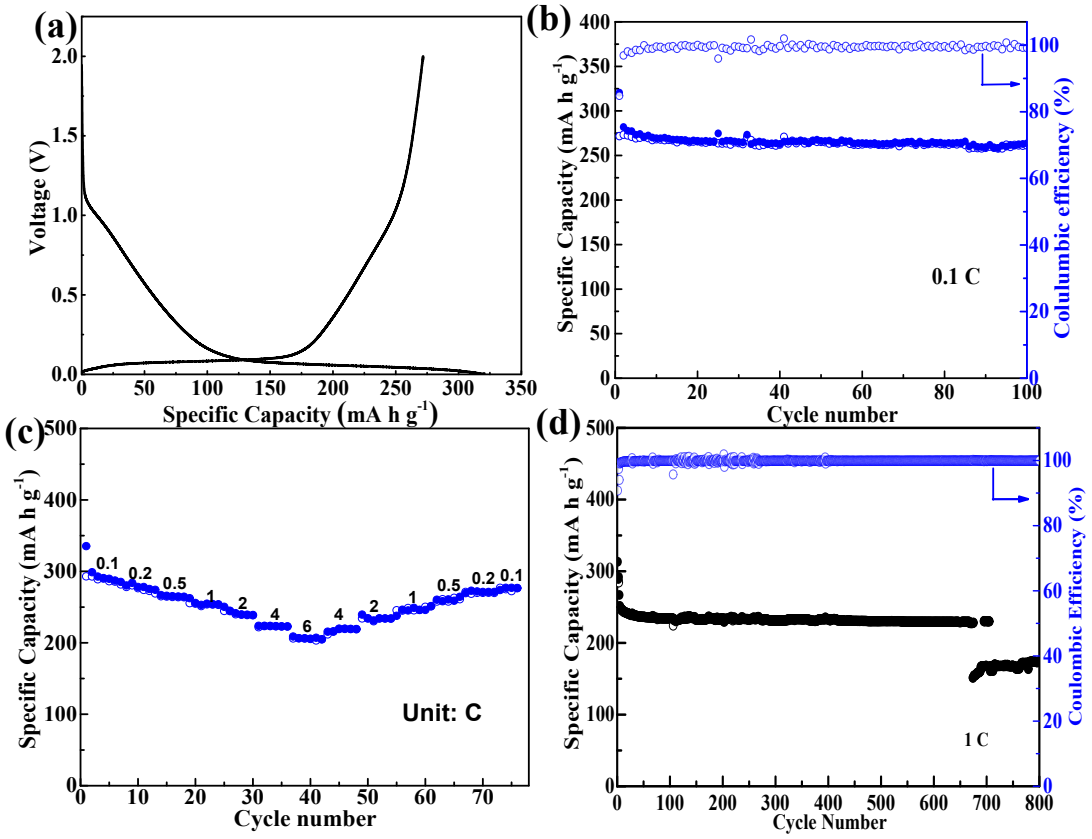

Fig. S9 Electrochemical performance of carbon-coated hard carbon from phenolic resin without nitrogen-doping: (a) Initial galvanostatic charge/discharge curves at 0.1 C; (b) Cycling performance at 0.1 C; (c) Rate performance from 0.1 C to 6 C; (d) Long-term cycling stability at 1 C.

To further study the application feasibility of HC@C for SIBs, the HC@C anode

was matched with $Na_3V_2(PO_4)_3$ cathode to assemble sodium full batteries. Prior to the full battery fabrication, the HC@C anode was presodiated to further eliminate the irreversible sodium loss. The battery was cathode limited, with the capacity ratio of anode to cathode around 1.5:1. The current density and the specific capacity of the full battery were calculated based on the mass of the cathode materials. The energy density of the full battery was calculated based on the mass of the cathode and anode materials. The full battery was cycled between 2-4.3 V. As shown in Fig. S10, the full battery fabricated with the $Na_3V_2(PO_4)_3$ cathode and presodiated HC@C anode shows the ICE of 94%. The full battery delivers an average working voltage of 3.15 V and the reversible capacity stays around 96 mA h g^{-1} after 100 cycles at 0.1 C, corresponding to the energy density of 230 W h kg^{-1}. When the current density increases to 10 C, the reversible capacity maintains around 75 mA h g^{-1}. The HC@C anode with superior sodium storage performance endows the full battery with excellent electrochemical performance.

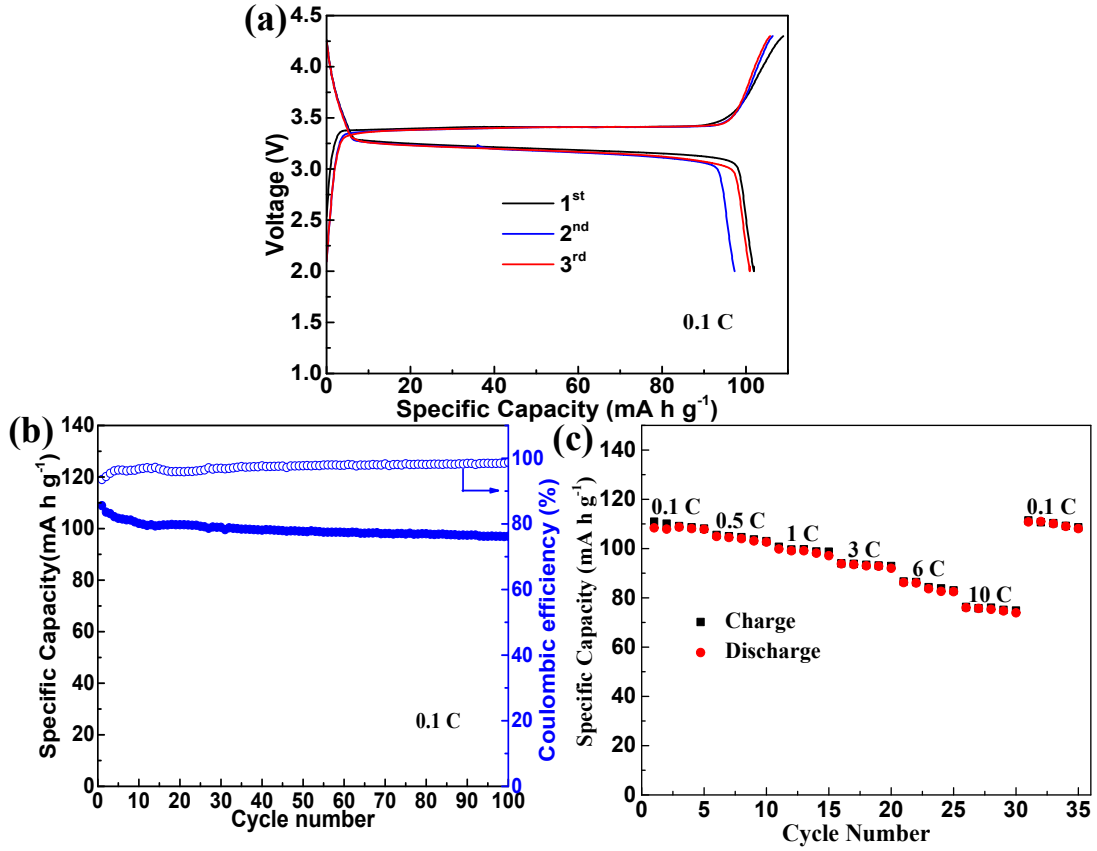

Fig. S10 Electrochemical performance of the full SIBs built with $Na_3V_2(PO_4)_3$ cathode and presodiated HC@C anode. (a) The galvanostatic charge/discharge curves of the full SIBs at 0.1 C

between 2-4.3 V during the initial three cycles; (b) Cycling performance of the full SIBs at 0.1 C; (c) Rate performance of the full SIBs at various current densities.

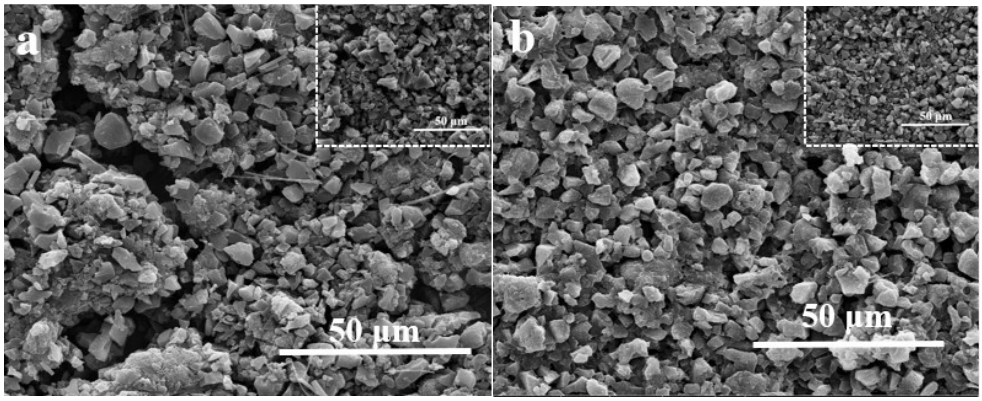

Fig. S11 SEM images of HC (a) and HC@C (b) anodes after 100 cycles under lower magnification. Inset: SEM images of the anodes before cycling.

The EIS results shown in Fig. S12a and Fig. S12b indicate that the resistances stem from the SEI films and charge transfer for the HC@C anode are much smaller than that of HC, further implying thinner SEI and faster sodium storage kinetics for the HC@C anode. As shown in the Raman spectra of Fig. S12c, the value of I_D/I_G for the HC anode increases from 1.07 to 1.21 after 100 cycles, whereas the I_D/I_G value shows little change and maintains about 1.13 for the HC@C anode after 100 cycles, demonstrating its more stable interface structure.

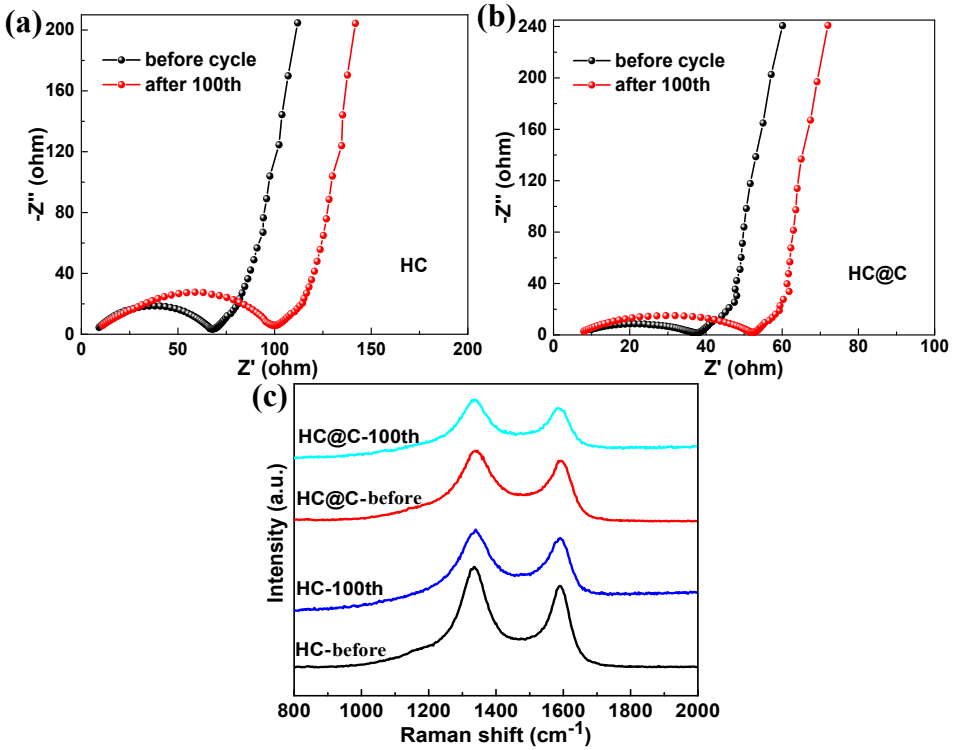

Fig. S12 EIS analysis for HC (a) and HC@C anodes (b) before and after 100 cycles; Raman spectra (c) of HC and HC@C anodes before and after 100 cycles.

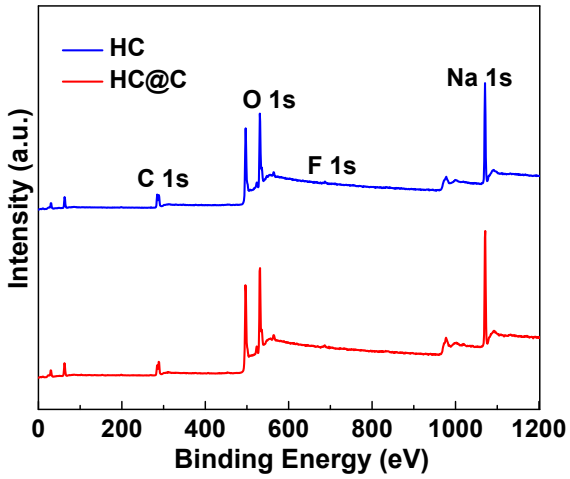

Fig. S13 The full XPS spectra of HC and HC@C anodes after 100 cycles.

Table S2 The corresponding species ratios of C1s XPS spectra.

	SP^2C/%	C=C/%	C-H/%	C-O/%	RCH_2Na/%
HC	11.2	16.1	15.4	9.8	47.5

HC@C	12.6	15	8.9	5.5	58

Table S3 The corresponding species ratios of O 1s XPS spectra.

	Na_2O/%	C=O/%	C-O/%	RCH_2ONa/%
HC	27.3	17	39.6	16.1
HC@C	32.3	19.5	32.6	15.6

Table S4 The corresponding species ratios of F 1s XPS spectra.

	Na-F/%	P-F/%
HC	16.1	83.9
HC@C	22.2	77.8